Review of photonic Hilbert transformers

Chaotan Sima, James C. Gates, Michalis N. Zervas, and Peter G.R. Smith

Optoelectronics Research Centre, University of Southampton,

Southampton SO17 1BJ, United Kingdom

Abstract

This paper reviews the demonstrations of photonic Hilbert transformers, describing their progress and recent developments. The physical operating principles of photonic Hilbert transformers including fractional Hilbert transformers are discussed, together with device applications in all-optical signal processing. Versatile approaches to realize photonic Hilbert transformers are discussed, e.g. discrete free space optics, fiber-based schemes and integrated planar geometry. The numerical designs and experimental performances of these photonic Hilbert transformers are analyzed in terms of spectral quality, operating bandwidth, system integration, and mechanical and thermal stability. Recent developments of the monolithically integrated photonic Hilbert transform devices include directional couplers and planar Bragg gratings which allow all-optical single sideband suppression and sideband switching.

Introduction

Transform techniques are widely used in various areas of mathematics, science, and engineering, one of which is the principal integral transform perhaps best known as the Fourier transform. The Hilbert transform (HT) sits alongside Fourier transforms amongst these integral transforms.

David Hilbert defined a pair of integral equations which connected the real and imaginary parts of a function analytic in the unit disc, which leads to the definition of the Hilbert transform on the circle [1]. The definition was believed to be first discussed by G. H. Hardy and named by him in 1924 as the Hilbert transform, in honor of Hilbert's contribution. Alfred Tauber, Titchmarsh and Young have made substantial contributions to establish the transform. A more complete historical discussion can be found elsewhere [1]. The definitions of the Hilbert transform as well as the fractional Hilbert transform (FrHT) are included in the later sections.

Over the decades, Hilbert transformations have had widespread use as they can be applied in the theoretical descriptions of many devices and systems and directly implemented in the form of analog or digital filters (Hilbert transformers) [2]. There are various optical implementations for spatial HTs and FrHTs [3-14]. It was first demonstrated in 1950 by Kastler [3] for image processing, especially for edge enhancement, and Wolter [4] for spectroscopy. Later the HT processor was made achromatic [5], two dimensional [6], and angularly isotropic [7]. The achromatic version is based on the detour phase concept, which became the origin of synthetic complex spatial filters [8] and of computer-generated holograms [9]. The spatial FrHT was also demonstrated to improve the performance of conventional HT and allow an additional degree of freedom [10, 11]. Further applications in spectroscopy and image process have also been presented [12-14].

More recently, with the development of optical communication technology and integrated optics, photonic Hilbert transformers (PHTs) have been realized and utilized across the all-optical domain. These include optical fiber schemes [15-25], photonic integrated circuits [26-30], and the programmable Fourier domain optical processor (FDOP) [31]. These devices are rather promising in meeting the demand for direct processing of optical signals at high speeds and operational bandwidths, enabling future all-optical high performance networks.

This paper reviews the photonic Hilbert transform from basic principles to applications. We first mathematically define the HT and FrHT, and their physical properties. Through a review of recent PHTs, we provide comparisons between these existing demonstrations in terms of their operating principles, fabrication, system integration, experimental performance and further applications. Fabrication challenges are also discussed to realize the favorable performance of the proposed devices. We then present the integrated PHT based on planar Bragg gratings in silica-on-silicon substrates, with the most recent progress in realizing integrated applications. Finally, we give a brief summary and outlook of PHTs and their future applications.

Operation principles

This section defines the Hilbert transform in the temporal and frequency domain, and it has also been used in the spatial domain.

Definition of HT and FrHT

The conventional Hilbert transform H[g(t)] of a one-dimensional real signal g(t) is defined as [2]:

$$H[g(t)] = \hat{g}(t) = g(t) * \frac{1}{\pi t} = \frac{1}{\pi} P \int_{-\infty}^{\infty} \frac{g(\tau)}{t-\tau} d\tau \tag{1}$$

where P stands for the Cauchy principal value of the integral to make the defined integral exist, which is obtained by considering a finite range of integration that is symmetric about the point of singularity. Detailed discussion of the Cauchy principal value is presented in [2]. The symbol * denotes the convolution of g(t) and$1/\pi t$.

The Fourier transform of the kernel of the Hilbert transformation is

$$H[g(\omega)] = \hat{g}(\omega) = -j\,\mathrm{sgn}(\omega) g(\omega) \tag{2}$$

where ω is the angular frequency. The sign function sgn(ω) is defined as follows:

$$\mathrm{sgn}(\omega) = \begin{cases} +1 & , \quad \omega > 0 \\ 0 & , \quad \omega = 0 \\ -1 & , \quad \omega < 0 \end{cases} \tag{3}$$

Equation (2) can be simplified as

$$H(\omega) = -j\,\mathrm{sgn}(\omega) \tag{4}$$

When a conventional HT is generalized into a FrHT, the frequency version of $H_{Fr}(\omega)$ is given by [1]

$$\begin{aligned} H_{Fr}(\omega) &= \begin{cases} e^{-j\varphi} & , \quad \omega > 0 \\ \cos(\varphi) & , \quad \omega = 0 \\ e^{j\varphi} & , \quad \omega < 0 \end{cases} \\ &= \cos(\varphi) + \sin(\varphi) \cdot [-j\,\mathrm{sgn}(\omega)] \\ &= \cos(\varphi) + \sin(\varphi) \cdot H(\omega) \end{aligned} \tag{5}$$

where $\varphi = \rho\pi/2$ and ρ indicates the fractional order. The formula shows that the FrHT of a signal is a weighted sum of the original signal and its conventional HT. This also expresses that the frequency response of Hilbert transform has a $(\rho\pi/2)$ phase shift at ω=0 while the amplitude remains constant. The FrHT becomes the conventional HT when ρ=1 and it offers no modification to the input signal when ρ=0 or ρ=2. The HT can be regarded as a process that phase shifts the input signal by $-\pi/2$ in the temporal domain prior to a defined temporal position and by an angle of $+\pi/2$ post this temporal position. It is conventional to interpret the transform in the frequency domain and Fig. 1(a) shows the complex frequency response of the HT and FrHT functions. Figure 1 (b) illustrates the amplitude (blue solid line) responses of the HT and FrHT functions with Fig. 1 (c) showing the phase response of the HT (red sold line) and a ρ order FrHT (red dashed line). The amplitude responses of HT and FrHT are identical.

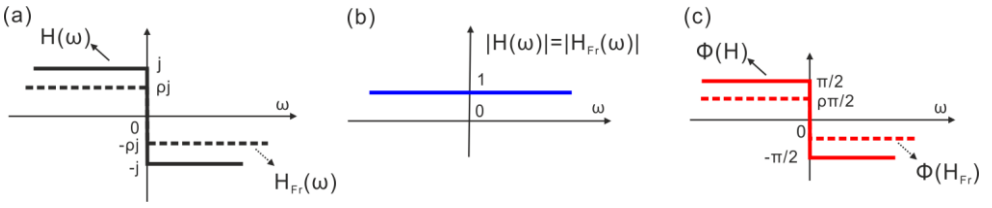

Fig. 1(a) Theoretical expression of the HT (solid line) and FrHT (dashed line) functions; (b) the amplitude and (c) phase responses of the HT (solid line) and the ρ order FrHT (dashed line).

2.2 Causality and realizability

Causality is the relationship between cause and effect [32]. A system is causal if h(t) = 0 for t < 0, where h(t) denotes the system impulse response. The ideal Hilbert transformer is non-causal and physically unrealizable. In any practical implementation of the Hilbert transformer, the output signal is a delayed and somewhat distorted HT of the input signal. The Paley-Wiener theorem [2] provides the necessary and sufficient conditions that a frequency response characteristic must satisfy, for the resulting filter to be causal and finite. As a consequence the frequency response of the HT will be band-limited with a bandwidth Δf and smooth alteration in phase as illustrated in Fig. 2.

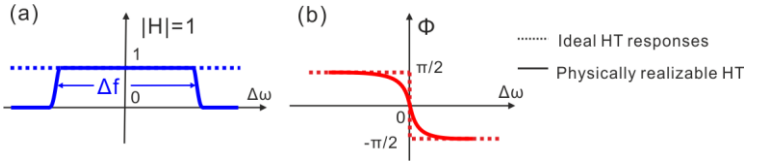

Fig. 2 Schematic drawing of the (a) amplitude and (b) phase responses of a physically realizable HT (solid lines) compared to those of the ideal HT (dashed lines) in the frequency domain.

Consequently, the physically realizable HT filter is a practical band-pass filter with a π phase shift (fractional π for FrHT) in the central frequency (Δω = 0). Apart from electronic Hilbert transformers [2], different theoretical and experimental approaches of PHTs are discussed and analyzed in the next sections. Figure 3 shows the block diagram of the interferometric all-optical single-sideband (SSB) modulation system, a crucial application of PHT, which were experimentally demonstrated in fiber schemes [15, 18, 19, and 25]. An optical attenuator, delay line and a phase shifter are incorporated in the system to balance the optical path and signal phases for coherent operations.

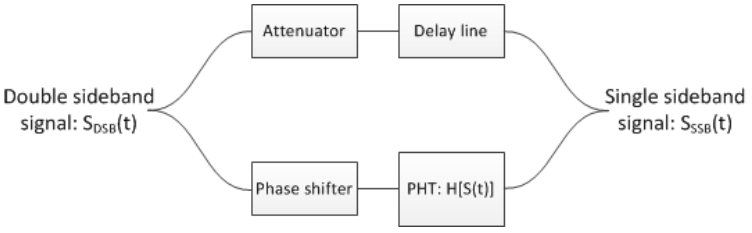

Fig. 3 Block diagram of the all-optical SSB modulation system using PHT.

Optical implementations of PHT

In the past half century, various research groups have published investigations and utilizations of PHTs for spectroscopy, optical signal processing, microwave photonics and radio over fiber systems, etc. These efforts have produced PHTs and FrHTs in free space objects [3-14], optical interferometers and delay lines [11-18], sampled FBGs [19], and phase-shifted FBGs with appropriate apodization profiles [20-25], integrated platforms [26-30] and the FDOP wave-shaper [31]. Considering the PHT implementations in signal processing, single-sideband (SSB) modulation is a well-known technique for improving performance in terms of required power, enhancing spectral efficiency and reducing fading [25]. Electronically, Hilbert transformers have been widely used in terms of analytical functions in SSB modulation applications with analogue and digital format [2]. In this section, the characteristics of these demonstrations and examples on SSB applications are briefly reviewed.

Free space

Early demonstrations of PHT have been reported since 1950 using free space lenses and plates [3-10]. Figure 4 shows the original optical setup used by Kastler [3] and Wolter [4]. They employed a conventional optical spatial filter with a filter

that consisted of a glass plate half covered by a π phase-shifting layer. The output image O(x) was the Hilbert transformation of the input image I(x) that had a π phase-shift at $s \geq 0$ and remained unmodified at $s \leq 0$.

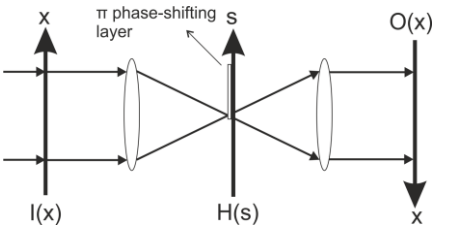

Fig. 4 Optical setup for performing the conventional spatial HT and FrHT (reprinted from [10]).

As mentioned above, the FrHT of a signal is a weighted sum of the original signal and its conventional HT. Here, the weighting parameters cos(φ) and sin(φ) in Eq.(5) are varied simply if the object signal is linearly polarized at 45º, if the filter consists of two pieces of a quarter-wave plate (oriented at 0º for $\omega \geq 0$ and at 90º otherwise). The output polarizer is oriented at angle φ, the magnitude of which controls the weighting parameter. Furthermore, Lohmann et al. proposed some other approaches which combined HTs with fractional Fourier transforms [10] and realizing two dimensional FrHTs [11].

The free-space implementation of PHTs has been proposed in many application areas, such as spectroscopy and image processing [12-14]. Nevertheless, in signal processing and telecoms, the PHT and FrHT in free space setups are no longer suitable, as they suffer from the limitations of bandwidth, response time, system stability etc. With the development of fiber technology and integrated optics, alternative approaches have been investigated in the last decade.

Non-grating-based fiber schemes

In fiber-related schemes, Hilbert transforms as well as FrHTs have been proposed and demonstrated via: Mach-Zehnder Interferometers (MZIs) with optical delay lines [15], transversal filters with wavelength division multiplexing (WDM) techniques [16, 17], and photonic microwave delay-line filters [18].

Figure 5 presents the impulse responses of HTs and configurations of the proposed all-optical HT by Tanaka et al [15]. Their all-optical different order (viz. fractional) Hilbert transformers were realized by combinations of several fiber-based MZIs and optical delay lines, shown in Fig. 5(a). Different delays of optical signals resulted in the corresponding impulse responses which were rotated at the tap center, as shown in Fig. 5(b). Figure 5(c) shows the fiber-based system using the HT system in Fig. 5(a) for SSB implementations. The sideband suppression scenario with 7.8 dB ratio was exhibited in Fig. 5(d). The SSB suppression ratio was defined as the ratio between the power of the unwanted sideband and the desired one. This work demonstrated the first PHTs used for single sideband applications in an all-optical scheme. It was realized by the concatenation of MZIs, tunable delay lines (D-line), the optcial attenuator (ATT), the polarization controller (PC), optical couplers as well as phase shifters, resulting in a complex optical system, which cannot be easily integrated or put in a compact form.

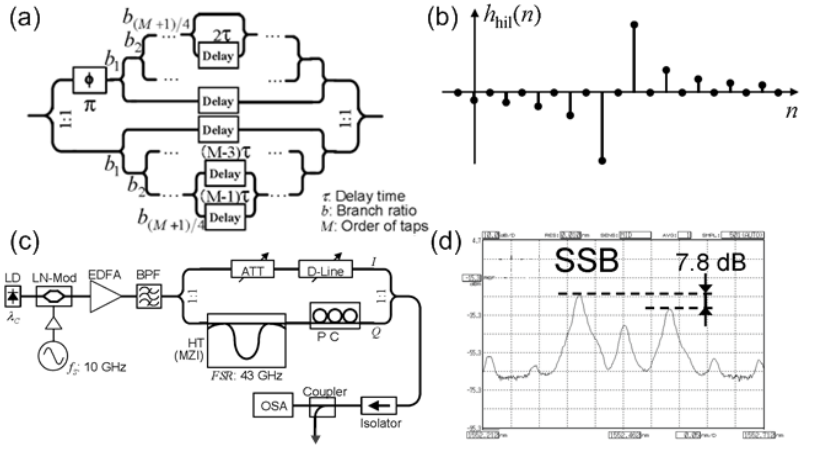

Fig. 5 Configuration of a non-grating fiber based PHT (a) method combining several fiber-based MZIs to form the PHT; (b) impulse response of PHT in (a);(c) experimental setup of optically phase-shifted SSB modulation using (a);(d) SSB signal with 7.8 dB suppression ratio at 10 GHz of system in (c) (reprinted from [15]) .

In 2008, Emami et al. demonstrated a RF Hilbert transform using all-optical schemes with a four-tap transversal filter and a coarse WDM coupler [16, 17]. The PHT configuration and RF generation are shown in Fig. 6. Measured and simulated data of PHT responses were shown in Fig. 6(b) and 6(c). The amplitudes and delay times of optical signals (wavelengths of λ_1 - λ_4) were empirically adjusted and located at desired wavelength intervals, with necessary time spacing [16]. A 90° phase shift with 3 dB of amplitude ripple was obtained within a 2.4 - 17.6 GHz bandwidth. However, some degradation of the performance above 20GHz was apparent. This system was modified into a two-tap transversal filter with an additional reference tap, providing two orthogonal DC measurements to perform simultaneous frequency and power measurement [17]. The manipulation of signals with different wavelengths was critical and empirical. In such a system, the operational bandwidth and adaptability were inevitably restricted.

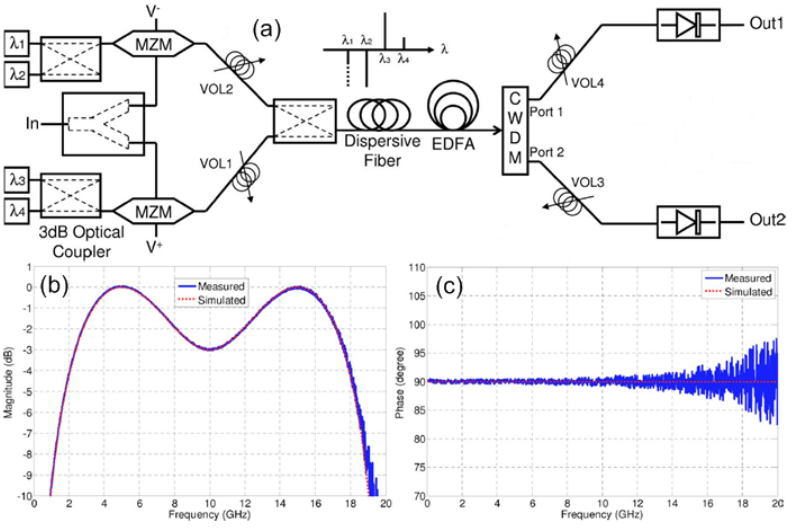

Fig. 6(a) System implementation with pre-setting 4 taps weights and spacing; (b) magnitude response; (c) phase response (reprinted from [16]).

In 2011, Huang et al. applied the programmable Fourier domain optical processor (FDOP, Finisar® WaveShaper) and high-speed photodiodes as a PHT for a microwave photonic quadrature filter [31]. The wave-shaper is a wavelength selective switch, and also permits reconfigurable per-channel dispersion trimming. Advantageous responses were reported with < 0.23 dB amplitude and < 0.5° phase imbalances. Nonetheless, the wave-shaper system is costly and lack of long term stability.

In 2012, Yao et al. reported microwave delay line filters for PHTs, which were also used as first-order microwave differentiators [18]. They implied PHTs with the bandwidth of ~24 GHz in microwave photonic operations with advantages of arbitrary wavelength operation and tunable responses. Chromatic dispersion related signal power fading in the dispersive fiber for wider operation bandwidth and system stability are yet to be concerned.

In view of operation principles and demonstrations, there are some similarities among the non-grating-based fiber schemes mentioned above. Precise controls of magnitude and delay time for each wavelength tap are essential for PHT operation. Many components such as MZIs, fiber couplers, optical delay lines and dispersive fibers are necessary and should be adjusted individually for optimal performance. In these systems, coupling loss, environmental effects, high system costs, thermal and mechanical stability as well as adjustability limit the performance and practicality of these approaches.

Fiber Bragg gratings

Fiber Bragg gratings (FBGs) have developed into a critical component for many applications in fiber-optic communication and sensor systems [33]. The spectral characteristics of FBGs represent amplitude and phase modulation of the input optical signal, which could incorporate Hilbert transform features all-optically. Since 2007, PHTs designed with sampled FBGs [19], using the space-to-frequency-to-time mapping (SFTM) algorithm [20, 21] and inverse scattering methods (also called discrete layer peeling) [22-25] were reported consecutively.

In 2007, Hanawa et al. reported experimental demonstrations of PHTs with sampled FBGs [19]. Figure 7 shows the sampled FBG design, its responses, the schematic of the optical SSB generation filter and SSB response. Beside the sampled FBG, the uniform FBG (UFBG) was introduced in one arm of the couplers. The optical attenuator (ATT), the tunable delay line (TDL) and the polarization maintaining couplers were included in the PHT schemes. The sideband suppression ratio about 10 dB with the bandwidth of 15 GHz was obtained. The ratio was lower than the simulated data due to the non-ideal responses of the various optical components [19]. The bandwidth of the system was limited as a consequence of the discrete apodization envelope; this is difficult to overcome using conventional phase mask FBG

inscription techniques. The authors comment in the paper that the SSB filter performance is sensitive to the optical phase and state-of-polarization of the interrogation source. This is likely to originate from the imbalanced nature of the interferometer, which when using discrete fiber components is challenging to overcome.

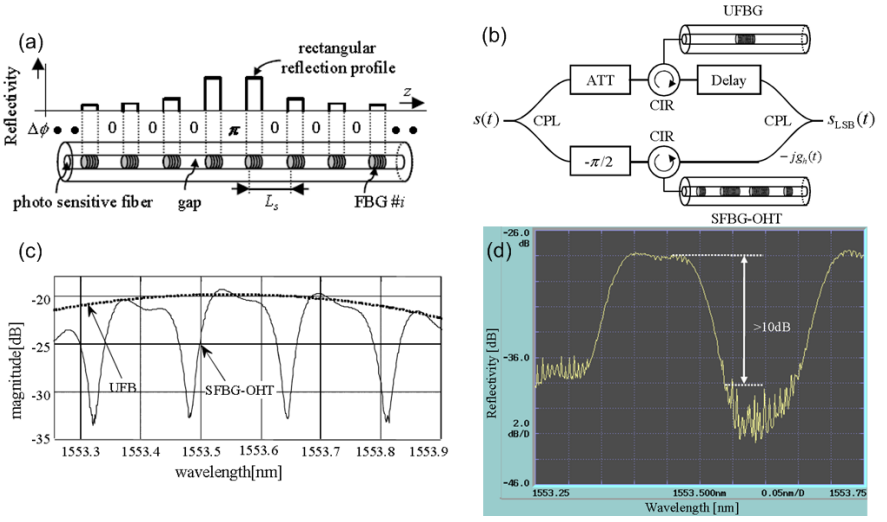

Fig. 7(a) Sampled FBG design; (b) the schematic of the optical SSB generation filter; (c) reflection spectral of the both arms; (d) sideband suppression characteristic of the optical SSB generation (reprinted from [19]].

In 2010, Yao et al. presented the theoretical design and experimental results of FBG-based PHTs using the inverse scattering method [22, 23]. Later in 2011 they reported PHT implementation in an optical SSB suppression system [25]. The FBGs were fabricated with apodization profiles and appropriate phase shifts, which were derived using the inverse scattering method. Figure 8 shows (a) the FBG design, (b) and (c) the fabricated grating responses, (d) the optical SSB modulation system setup, and (e) the generated optical SSB signals at different microwave frequencies. The tunable delay line (TDL), the polarization controller (PC), the couplers and the attenuator (ATT) are necessary in the setup. 15- 20 dB suppression ratios were achieved in the frequency bandwidth of 20 GHz. There were some drawbacks including performance degradation believed to be due to the non-ideal and not easily controllable π/2 phase shift in the upper MZI arm and the poor long-term stability owing to the wavelength drift of the FBG and the MZI [25]. External temperature compensation would be necessary to deal with this problem.

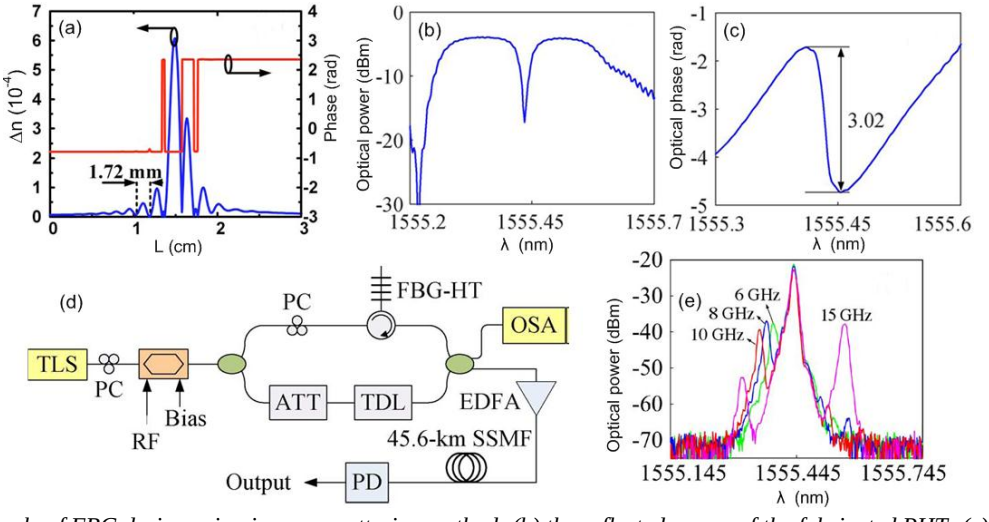

Fig. 8(a) An example of FBG design using inverse scattering method; (b) the reflected power of the fabricated PHT; (c) phase response of the fabricated PHT; (e) the SSB signal generation system;(d) generated signals (reprinted from [22, 32]).

By means of the space-to-frequency-to-time mapping algorithm, Asghari et al. simulated the conventional first order PHT [20] and Cuadrado extended it to fractional orders [21]. Grating apodization profiles were derived via inverse Fourier transform and SFTM, and the HT temporal and frequency responses were presented.

So far, the presented FBG-based PHT implementations suffer from rather small operation bandwidths (a few GHz), imposed by the FBG bandwidths. To overcome this limitation, long period gratings have been proposed and numerically designed to perform Terahertz bandwidth PHTs [24]. Apodized gratings with the 430 μm period and a single π phase-shift in the standard single-mode fiber (Corning SMF-28) platform were simulated using inverse scattering methods [34, 35], giving device operation bandwidths up to 18.37 THz.

Photonic integrated circuit

Despite the big performance improvements and experimental topology simplifications, efficient FBG incorporation into all optical PHT implementations still require optical circulators and fine optical and polarization adjustments. To ameliorate some of these problems, Bragg gratings have been experimentally demonstrated in the planar silica-on-silicon format [27] and implemented into monolithically integrated optical SSB modulators [28], which will be discussed in the following sections.

Integrated optics has seen rapid growth and significant development in the global optoelectronics market, since it was first proposed by S. E. Miller in 1969 [36]. Based on the unique features of the planar geometry, photonic integrated circuits (PIC), such as arrayed-waveguide gratings (AWGs), optical add/drop multiplexers (OADMs) and distributed-feedback lasers (DFBs), have been thoroughly investigated and commercialized in the last two decades [37]. Compared to fiber based schemes, planar waveguide devices can significantly reduce the system complexity, increase long term stability, and meet with the additional demands of volume manufacturability, compactness, ruggedness and low cost, all of which are essential for practical PHT deployment.

Tanaka et al. numerically proposed the PHT with branching waveguides for SSB signal suppression [26] and later Takano et al. experimentally realized it in fiber-based systems as shown in Fig. 5. The transformer was constructed by an optical phase shifter, three optical delay lines and branching waveguides including asymmetric structures.

Recently, Zhuang et al. proposed and experimentally established a photonic on-chip implementation of FrHT using ring resonator-based optical all-pass filters [29, 30]. The optical ring resonator (ORR) and the MZI were used to implement PHTs, shown in Fig. 9(a). The MZI here was structured to close the ring path, which served as a practical tunable power coupler. The impulse response of the ORR was illustrated in Fig. 9(b). The phase response and the power transfer of the fabricated device are shown in Fig. 9(c) and 9(d) respectively. This device features the variable and arbitrary fractional order of the Hilbert transformer, space efficiency and compatibility for large-scale integration. Nevertheless, the fabrication of such devices requires high precision to ensure the correct phase and operation wavelength, in reality heater assemblies are used post trimming of the devices. Some of the disadvantages of the ORR device come from the intrinsic material properties which result in high sensitivity to environment conditions such as temperature and mechanical stress. As a consequence these devices suffer the drawbacks of limited long term stability and mass reproducibility.

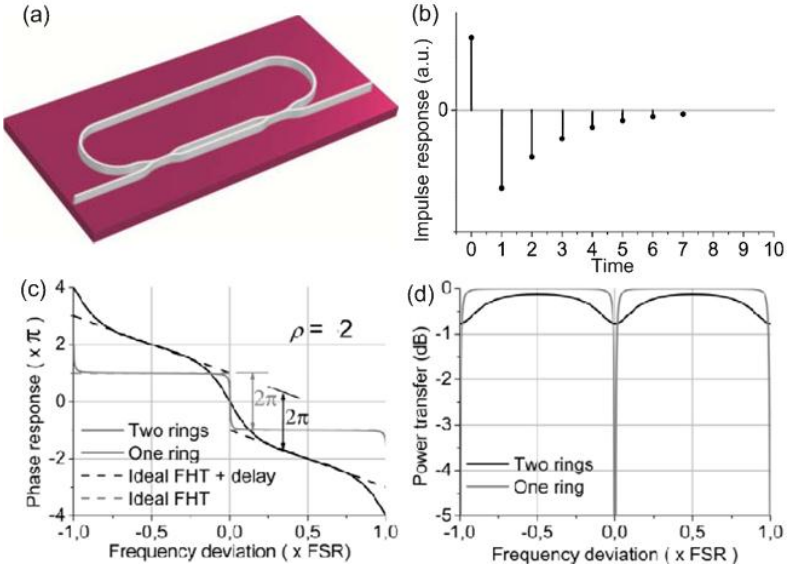

Fig. 9(a) Schematic of one ORR with MZI; (b) the impulse response of the ORR; (c) phase response and (d) power transfer of the FrHT using one ORR and another FrHT using two cascaded ORR. ρ indicates the fractional order (reprinted from [29]).

Planar Bragg grating

To overcome the complexity and increased environmental sensitivity of fiber-based implementations and previously reported integrated circuits, a silica based integrated circuit employing Bragg gratings was presented in 2011 [27]. Later this work was extended to a monolithically integrated all-optical SSB modulation device [28], as shown in Fig. 10. The PHT was implemented using a planar Bragg grating with appropriate apodization profile and a π phase shift within the grating. Direct UV grating writing technique (DGW) [38] was used to fabricate the device, as a flexible and powerful tool to manipulate arbitrary Bragg grating structures without the need for phase masks.

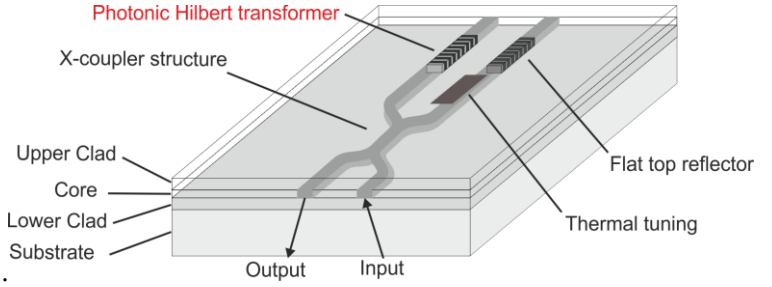

Fig. 10 Schematic of the proposed integrated SSB modulation device with a planar Bragg grating based PHT, located in a single silica-on-silicon chip.

The grating refractive index modulation Δn is shown in Fig. 11(a), derived from the SFTM method [15]. The preliminary data of the reflectivity and relative group delay of the PHT grating were presented in Fig. 11(b) and 11(c) respectively [27]. With the improvement of the DGW technique [38], the grating responses become more perfect, with nearly flat top power reflection (~1dB ripples and ~200 GHz bandwidth), as shown in Fig. 11(d).

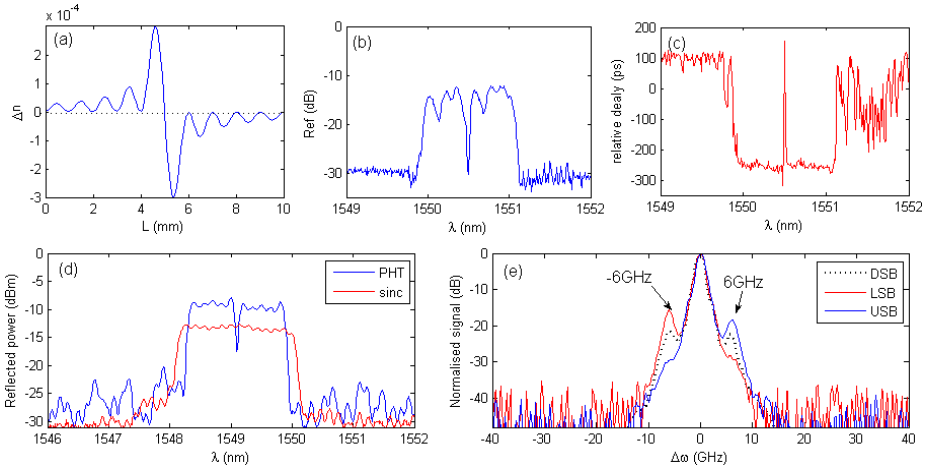

Fig. 11(a) The grating refractive index modulation profile; (b) reflectivity spectrum of the initial PHT grating; (c) relative group delay response of the initial PHT grating [27]; (d) The amplitude responses of another improved PHT grating (blue) and the sinc-apodized flat top reflector (red); (e) all-optical SSB generation and switching, compared with the double sideband (DSB) signal[28].

Considering the PHT implementations in all-optical SSB filters, the silica-on-silicon planar format was employed, composed of an X-coupler, a PHT, a flat top reflector and a micro heater. Sinc-apodized Bragg grating was utilized as the flat top reflector. The reflected optical signal from the two gratings undergoes constructive and destructive interference, thereby suppressing one side band and enhancing the other. The relative optical phase of the two signals was determined by the relative position of the gratings which was further fine-tuned by a small micro heater present on one arm of the device. As shown in Fig. 11(e), the 12dB single-sideband suppression ratio and side band switching at 6 GHz microwave frequency were demonstrated [28]. In the experiments, this device had the benefits of integrated single structures, direct thermal tuning, balanced optical path, fiber compatibility, long term thermal stability and could be used alongside conventional etched silica-on-silicon devices. The operative bandwidth of the data presented was limited by the available characterization equipment and not the device. Stronger PHT gratings and greater SSB suppression could be achieved by improving phase trimming and inverse scattering methods. The precision of the fabrication techniques should also allow the manipulation of devices without the need for active phase control.

Summary

Major experimental implementations are summarized and listed in Table 1, corresponding to the presented data and figures in the literatures. The device operative bandwidths, fabrication simplicity and system stability are estimated form the presented data and statement. In [31], the key component FDOP is the commercial product Finisar® wave-shaper for which a description of fabrication process is not applicable.

Table 1 Comparisons between current PHT implementations

Researchers	Operation principle	Device response quality	Device operation bandwidth (GHz)	Fabrication simplicity	System stability	Application
Takano et al.	MZI + delay line	√	10	√	√	SSB ratio: 7.8 dB
Emami et al.	transversal filter + coarse WDM coupler	√	20	√	√	Frequency measurements
Hanawa et al.	Sampled FBGs	√√	15	√	√	SSB ratio: > 10 dB
Huang et al.	FDOP + photodiodes	√√√	100	N.A.	√	Quadrature RF signal generation
Yao et al.	Photonic microwave delay line filters	√√	24	√√√	√	Differentiator
Yao et al.	Single FBG	√√	100	√√	√	SSB ratio: ≤ 20 dB
Zhuang et al.	MZI + optical ring resonator	√√√	10	√√	√√	Quadrature RF signal generation
Sima et al.	Integrated planar Bragg grating	√√√	200	√√√	√√√	SSB ratio: ≥ 12 dB

N. A.: Not applicable.

Conclusion and outlook

The past decade has witnessed exciting progress in the field of photonic Hilbert transformers with the development of fiber technology and integrated optics. Owning to their enormous advantages such as operational bandwidths and speeds far beyond current electronic technologies, PHTs have been attracting more and more attention in recent years. However, fabrication challenges and system stability issues still remain, particularly considering the high speed operations in all-optical signal processing. For those in optical communications and optical computing, processed optical signals in terms of optical phase and central wavelength would be rather sensitive to environmental effects. These concerns have raised great challenges and opportunities for future research on PHTs. Grating based and non-grating based systems in integrated formats are both attractive due to simple and compact structures, and the preferable choice depends on the fabrication technology. Integrated multi-functional PHT devices with are promising and prominent for future implementation and commercialization.

Acknowledgments

This work was supported by Engineering and Physical Sciences Research Council (EPSRC), University of Southampton, UK, and China Scholarship Council, China.

References

1. Frederick W K. Hilbert Transforms. Volume 1. Cambridge: Cambridge University Press, 2009, 1:1-7.
2. Hahn S L, Poularikas A D. The Transforms and Applications Handbook. 2nd Edition. Boca Raton: CRC Press, 2000, 7:1-18.
3. Kastler A. Un système de franges de diffraction à grand contraste. Review Optik. 1950, 29: 307–314.
4. Wolter H. Die Minimumstrahlkennzeichnung als Mittel zur Genauigkeitssteigeru ng optischer Messungen und als methodisches Hilfsmittel zum Ersatz des Strahlbegriffes. Annalen der Physik. 1950, 442 (7): 341–368.
5. Hauk D, Lohmann A W. Minimumstrah1ke.nnich- nung bei Gitterspektrographen. Optik. 1958 15: 275-281.
6. Lowenthal S, Belvaux Y. Observation of phase objects by optically processed Hilbert transform. Applied Physics Letters. 1967, 11 (2): 49–51.
7. Eu J K T, Lohmann A W. Isotropic Hilbert spatial filtering. Optics Communications. 1973, 9 (3): 257-262.
8. Brown B R, Lohmann A W. Complex spatial filtering with binary masks. Applied Optics. 1966, 5 (6): 967-969.
9. Lohmann A W, Paris D P. Binary Fraunhofer holograms, generated by computer. Applied Optics. 1967, 6 (10): 1739-1748.
10. Lohmann A W, Mendlovic D, Zalevsky Z. Fractional Hilbert transform. Optics Letters. 1996, 21 (4): 281-283.
11. Lohmann A W, Tepichín E, Ramírez J G. Optical implementation of the fractional Hilbert transform for two-dimensional objects. Applied Optics. 1997, 36 (26): 6620-6626.
12. Davis J A, McNamara D E, Cottrell D M, Campos J. Image processing with the radial Hilbert transform: theory and experiments. Optics Letters. 2000, 25 (2): 99-101.
13. Guo C, Han Y, Xu J, Ding J. Radial Hilbert transform with Laguerre-Gaussian spatial filters. Optics Letters. 2006, 31 (10):1394-1396.
14. Bokor N, Iketaki Y. Laguerre-Gaussian radial Hilbert transform for edge-enhancement Fourier transform x-ray microscopy. Optics Letters. 2009, 17 (7): 5533-5539.
15. Takano K, Hanzawa N, Tanji S, Nakagawa K. Experimental demonstration of optically phase-shifted SSB modulation with fiber-based optical Hilbert transformers. In: Proceedings of Optical Fiber Communication and the National Fiber Optic Engineers Conference, 2007, 1-3.
16. Emami H, Sarkhosh N, Bui L A, Mitchell A. Wideband RF photonic in-phase and quadrature-phase generation. Optics Letters. 2008, 33 (2):98-100.
17. Emami H, Sarkhosh N, Bui L A, Mitchell A. Amplitude independent RF instantaneous frequency measurement system using photonic Hilbert transform. Optics Express. 2008, 16 (18): 13707-13712.
18. Han Y, Chi H, Zhang X, Yao J. A continuously tunable microwave fractional Hilbert transformer based on a nonuniformly spaced photonic microwave delay-line filter. Journal of Lightwave Technology. 2012, 30 (12): 1948-1953.
19. Wang X, Hanawa M, Nakamura K, Takano K, Nakagawa K. Sideband suppression characteristics of optical SSB generation filter with sampled FBG based 4-taps optical Hilbert transformer. In: Proceedings of the 15th Asia-Pacific Conference on Communications, 2009, 622-625.
20. Asghari M H, Azaña J. All-optical Hilbert transformer based on a single phase-shifted fiber Bragg grating: Design and analysis. Optics Letters. 2009, 34 (3): 334–336.
21. Cuadrado-Laborde C. Proposal and design of a photonic in-fiber fractional Hilbert transformer. IEEE Photonics Technology Letters 2010, 22 (1): 33-35.
22. Li M, Yao J. All-fiber temporal photonic fractional Hilbert transformer based on a directly designed fiber Bragg grating. Optics Letters. 2010, 35 (2): 223–225.
23. Li M, Yao J. Experimental demonstration of a wideband photonic temporal Hilbert transformer based on a single fiber Bragg grating," IEEE Photonics Technology Letters. 2010, 22 (21): 1559-1561.
24. Ashrafi R, Azaña J. Terahertz bandwidth all-optical Hilbert transformers based on long-period gratings. Optics Letters, 2012,37(13): 2604-2606.
25. Li Z, Chi H, Zhang X, Yao J. Optical single-sideband modulation using a fiber-Bragg-grating-based optical Hilbert transformer. IEEE Photonics Technology Letters. 2011, 23 (9): 558-560.
26. Tanaka K, Takano K, Kondo K, Nakagawa K. Improved sideband suppression of optical SSB modulation using all-optical Hilbert transformer. Electronics Letters. 2002, 38 (3): 133–134.
27. Sima C, Gates J C, Rogers H L, Holmes C, Zervas M N, Smith P G R. Integrated all-optical SSB modulator using photonic Hilbert transformer with planar Bragg gratings. In: Proceedings of the European Conference on Lasers and Electro-Optics and the XIIth International Quantum Electronics (CLEO-EUROPE). Optical Society of America, 2011, paper CI4.5.

28. Sima C, Gates J C, Rogers H L, Mennea P, Holmes C, Zervas M N, Smith P G R. Continuously tunable integrated single-sideband modulator with photonic Hilbert transformer and planar Bragg gratings. Optics Letters. Under peer review.
29. Zhuang L, Beeker W, Leinse A, Heideman R, Roeloffzen C. Continuously tunable photonic fractional Hilbert transformer using ring resonators for on-chip microwave photonic signal processing. In: 2012 IEEE International Topical Meeting on Microwave Photonics (MWP2012), IEEE Photonics Society. Noordwijk, Netherlands, 2012, 1-4.
30. Zhuang L, Khan M R, Beeker W, Leinse A, Heideman R, Roeloffzen C. Novel microwave photonic fractional Hilbert transformer using a ring resonator-based optical all-pass filter. Optics Express, 2012, 20(24): 26499-26510.
31. Huang T H, Yi X, Minasian R A. Microwave photonic quadrature filter based on an all-optical programmable Hilbert transformer. Optics Letters. 2011, 36 (22): 4440-4442.
32. Proakis J G, Manolakis D G. Digital Signal Processing: Principles, Algorithms, and Applications, 4th Edition. New Jersey: Prentice Hall, 2007, 654-659.
33. Kashyap R. Fiber Bragg Gratings. 2nd Edition. San Diego: Academic Press, 2009.
34. Feced R, Zervas M N. Efficient inverse scattering algorithm for the design of grating-assisted codirectional mode couplers. The Journal of the Optical Society of America A. 2000, 17 (9): 1573-1582.
35. Brenne J K, Skaar J. Design of grating-assisted codirectional couplers with discrete inverse-scattering algorithms. Journal of Lightwave Technology. 2003, 21 (1): 254-263
36. Miller S E. Integrated Optics: An Introduction. Bell System Technical Journal. 1969, 48: 2059-2069.
37. Okamoto K. Fundamentals of Optical Waveguides. 2nd Edition. San Diego: Academic Press, 2006, 462-467.
38. Emmerson G D, Watts S P, Gawith C B, Albanis V, Riziotis C, Williams R B, Smith P G R. Fabrication of directly UV-written channel waveguides with simultaneously defined integral Bragg gratings. Electronics Letters. 2002, 38 (24): 1531–1532.